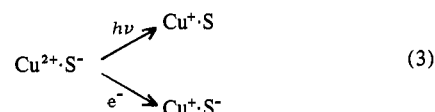


the lowest two charge-transfer states and an expected small energy gap between them¹⁵ supports the interpretation of the fast decay component as relaxation to the lower, $\pi S \rightarrow Cu d_{x^2-y^2}$, charge-transfer state. The crossing to the ground electronic state (eq 2) involves a larger rearrangement of ligands due to the change in electrostatic interaction between Cu and S and probably a larger energy gap and so is expected to be slower and rate determining. The observed 1.6 ± 0.2 -ps decay is thus interpreted as the reverse charge transfer, eq 2. The reverse charge-transfer process could also involve excited ligand field states of Cu^{2+} which lie lower in energy than the $\pi S \rightarrow Cu d_{x^2-y^2}$ charge-transfer state.³

Why is this rate of back charge transfer so fast? One might well ask why it is so slow. The Cu-S bond distance is about 2 Å,¹⁶ and a valence electron of typical energy requires about 10^{-16} s to travel from one atom to another. However, by charge transfer one means a transition from a state largely localized on one atom to a state largely localized on another. The rate of reverse charge transfer can be understood in the following way. The Cu-S vibration frequency is $1.2 \times 10^{13} s^{-1}$,³ and the rate of charge transfer is $(1.6 \times 10^{-12})^{-1} = 6.3 \times 10^{11} s^{-1}$. The probability of charge transfer during a vibrational period is the ratio of these two rates (i.e., ~ 0.05); this is about what one obtains by inserting typical parameters into the Landau-Zener formula for the probability of an allowed crossing from one electronic state to another during a collision. Alternatively, the reverse charge-transfer rate can be explained by using multiphonon models for electron transfer^{17,18} and a range of parameters typical for such models. Measurement of the reverse charge-transfer rate at other temperatures would be helpful in ascertaining the validity of these models and in fixing the parameters contained in them. The only previous measurement¹⁹ of a back charge-transfer rate was in an

aqueous solution of a diruthenium complex ion in which the electron was transferred between two ruthenium ions. The time measured was 2 orders of magnitude longer than that in azurin. The reason may be that solvent reorganization, absent in azurin, may cause a small increase in the potential barrier for electron transfer within the ruthenium complex.

The very fast spatial relaxation of the copper center implied by its very fast electronic relaxation has biochemical implications. In vivo, azurins and other proteins of its family exchange electrons with other metalloproteins, in particular, cytochromes. Rate constants found for this exchange²⁰ are in the range 5×10^5 – $4 \times 10^7 M^{-1} s^{-1}$. These rates are among the fastest known for protein electron-exchange reactions but are still one or more orders of magnitude slower than the rate of diffusion. The redox process involves a translational diffusion, a rotational diffusion so the proteins will fit in the best possible way, and a structural fluctuation which allows the two metal atoms to approach more closely than usual, followed by the electron jump. The change in electrostatic interaction between the Cu center and the cysteine S is larger upon excitation of the charge-transfer transition than when an external electron is captured by the Cu^{2+} and so the ligand rearrangement may be greater in the case of charge-transfer excitation (eq 3).



The picosecond experiment implies that the rearrangement of ligands around the Cu when its oxidation state changes is facile and is not rate determining for the electron transfer.

Acknowledgment. We gratefully acknowledge the technical assistance of D. J. Eilenberger. The Columbia investigators were supported by a grant from the National Institutes of Health, GM-19019.

(14) Shank, C. V.; Ippen, E. P.; Teschke, O. *Chem. Phys. Lett.* **1977**, *45*, 291.

(15) The potential surfaces for the $\sigma S \rightarrow Cu d_{x^2-y^2}$ and the $\pi S \rightarrow Cu d_{x^2-y^2}$ states should be similar due to the similar electron distributions. The difference between absorption maxima to the two states is $3000 cm^{-1}$ ³ and the energy gap between them should be comparable.

(16) Tullus, T. D.; Frank, P.; Hodgson, K. O. *Proc. Natl. Acad. Sci. U.S.A.* **1978**, *75*, 4069.

(17) Hopfield, J. J. *Proc. Natl. Acad. Sci. U.S.A.* **1974**, *71*, 3640.

(18) Jortner, J. J. *Chem. Phys.* **1976**, *64*, 4860.

(19) Creutz, C.; Kroger, P.; Matsubara, T.; Netzel, T.; Sutin, N. *J. Am. Chem. Soc.* **1979**, *101*, 5442.

(20) Wherland, S.; Pecht, I. *Biochemistry* **1978**, *17*, 2585.

Quenching of Pyrene Fluorescence by Single and Multivalent Metal Ions in Micellar Solutions

Franz Grieser* and Robert Tausch-Treml

Contribution from the Hahn-Meitner-Institut für Kernforschung Berlin GmbH, Bereich Strahlenchemie, D-1000 Berlin 39, Postfach, Germany. Received March 10, 1980

Abstract: The temporal characteristics of the quenching of pyrene fluorescence in micellar solution, by several metal ions, are shown to depend on the charge and type of metal ion. The quenching by Tl^+ and Ag^+ is pseudo-first-order and dependent on the micelle concentration. For bivalent metal ions the fluorescence quenching curves show a two-component decay behavior. The biexponential decay behavior is dependent on the micelle concentration, the ionic strength of the solution, and the bivalent ion used. It is shown that some of these effects can be accounted for by assuming that micelle-micelle collisions allow the transfer of a bound metal ion from one micelle to the other. Intracellular quenching constants were obtained for the quenching of excited pyrene by Cu^{2+} and Eu^{3+} ions in sodium dodecyl sulfate and sodium dodecyltrioxyethylene sulfate micelles and found to be dependent on both the metal ion and the micelle. From the experimental results it is also shown that bound metal ions are distributed among the micelles according to Poisson statistics.

Introduction

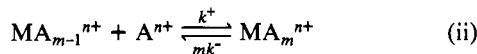
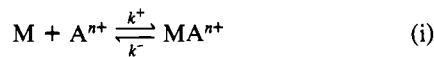
Ionic micelles, like charged colloids and ion-exchange resins, have the property of being able to bind oppositely charged ions. This aspect of micelles has been used in conjunction with their ability to solubilize hydrophobic molecules to study a variety of reactions. For example, it has been shown that adsorbed metal ions on anionic

micelles can act as efficient electron acceptors from excited micelle solubilized species,¹ can promote the rate of phosphorescence in some aromatic hydrocarbons,² and can "catalyze" metal/ligand

(1) (a) R. Scheerer and M. Grätzel, *J. Am. Chem. Soc.* **99**, 865 (1977); (b) S. A. Alkatis and M. Grätzel, *ibid.* **98**, 3549 (1976).

reactions in metal complex formation.³

Few kinetic studies however have been directed at studying the movement of metal ions in aqueous micellar solutions. In a simple scheme the reaction steps of importance are steps i and ii. The

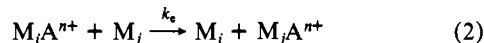


above steps represent the sequential binding of metal ions, A^{n+} , to the micelle, M . It is assumed that each association step is k^+ and the dissociation step mk^- , where m is the number of metal ions bound to the micelle.

The associated equilibrium constant is defined in eq 1, where $[MA^{n+}]_B$, $[M]$ and $[A^{n+}]_F$ represent the concentration of all the bound ions, the total micelle concentrations, and the unbound ions, respectively.

$$K = \frac{k^+}{k^-} = \frac{[MA^{n+}]_B}{[M][A^{n+}]_F} \quad (1)$$

Recently another process (eq 2) was suggested by Henglein and



Proske,⁴ that of bound ion movement through micelle-micelle collisions, where overlap of the ionic charge clouds of the colliding micelles allows the ion to migrate from one micelle to another. For Ag_2^+ bound to SDS micelles the above authors found that reaction 2 was relatively efficient with k_e equal to $2.8 \times 10^8 M^{-1} s^{-1}$.

In the present communication we present the results of a study on bound/free-ion movement for some single and multivalent metal ions in anionic micellar solutions. The quenching of fluorescence from micelle-solubilized pyrene by the metal ions and the reaction rate of the hydrated electron were the two techniques used to define the position of the bound ions and their exchange movements in the micellar solution.

Experimental Section

(i) **Materials.** Sodium dodecyl sulfate (SDS), BDH Ltd., specially purified grade, was recrystallized from 95% ethanol before use. The critical micelle concentration (cmc) from conductivity measurements was found to be $7.5 \times 10^{-3} M$ at 20 °C. The salts used were generally the sulfate salts of the metal ions, either Merck proanalysis or suprapure grade. Ultrapure $EuCl_3 \cdot 6H_2O$ was obtained from the Ventron Co. and Tl_2SO_4 (>99.5%) from Riedel-de Haen AG, Hannover, West Germany. These salts were all used as received. The water used was obtained from a millipore filtration system and had a conductivity of $<1 \times 10^{-6} \Omega^{-1} cm^{-1}$ and a pH between 6.0 and 6.4. Sodium dodecyl trioxyethylene sulfate ($C_{12}(EtO)_3S$) was a purified sample obtained from Henkel and Cie., Düsseldorf, West Germany. Pyrene, Eastman (99.99%), was recrystallized from ethanol and stored in the dark. Stock solutions of pyrene ($10^{-2} M$) were prepared in absolute ethanol (Merck, proanalysis). Microliter aliquots of this were injected into the surfactant solutions.

(ii) **Procedure.** Solutions containing pyrene ($\sim 4 \times 10^{-5} M$) were excited with 347.1-nm photons from a frequency doubled Korad KIQ switched ruby laser.⁵ The emission signals produced were monitored at right angles to the laser beam which was focused through a 380-nm cutoff filter and a monochromator and onto a 1P28 photomultiplier. The monochromator was set at 395 nm with a band resolution generally of 3–5 nm. The signal was then displayed on a Tektronix 7633 storage oscilloscope and photographed (3000 ASA polaroid film) for subsequent analyses. The time resolution of this setup was essentially limited by the

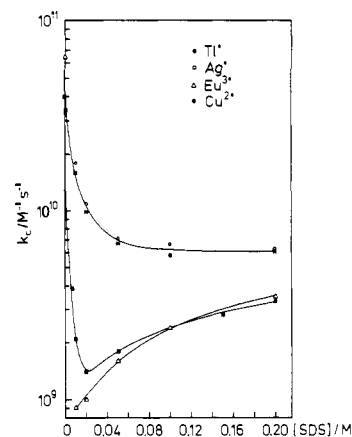


Figure 1. Apparent second-order rate constants for the reaction of the hydrated electron with metal ions in micellar solution. The concentrations of Ag^+ and Tl^+ were $5 \times 10^{-4} M$ (SO_4^{2-} was the counterion) and of Cu^{2+} and Eu^{3+} , $1 \times 10^{-3} M$ (counterions were SO_4^{2-} and Cl^- , respectively).

laser pulse width, 15–25 ns. The dose used to excite the pyrene in solution was sufficiently low that a two-photon ionization of pyrene,⁶ detected by the absorption of the pyrene cation at 453 nm, was effectively zero.

The reaction rate of the hydrated electron (e_{aq}^-) was measured by using the Hahn-Meitner-Institut Elbena electron accelerator system.⁷

Deoxygenated SDS solutions in the presence and absence of metal ions were irradiated with single, 5-ns pulses of ~ 4 MeV electrons. The decay rate of the hydrated electron was followed by its absorption at 600 nm, and the signal was recorded and processed by using a computer controlled system. Under the conditions used, the background decay rate ($t_{1/2}$) of the electron was 3–4 μs .

Solutions were deoxygenated by bubbling them with purified argon for $\sim 1/2$ h. Most of the solutions used in the pulse radiolysis and laser photolysis experiments were at a pH of 5.5–6.0 and were freshly prepared prior to the experiment. Some solutions were left for several days and, after being rebubbled with argon, gave the same results as when freshly made. An exception was the Fe^{2+} system which at a pH of ~ 6 showed a brown coloration in solution, presumably iron oxide, a few hours after preparation. To minimize the consequences of this effect we completed preparation and experimentation in $\sim 1/2$ h. Measurements were also made with solutions at pH 3.1 where the rate of brown coloration was considerably reduced. The results here were the same as those obtained at pH ~ 6 .

All measurements were made at room temperature, 20–23 °C.

Results and Discussion

(I) Reaction Rate of e_{aq}^- with Metal Ions in Micellar Solutions.

For some of the effects observed in the fluorescence quenching experiments, which are described in the following section, to be interpreted, the conclusions reached from the e_{aq}^- reaction rate data are important. These are therefore presented first.

The rate of reaction of e_{aq}^- with the metal ions in the surfactant solutions was monitored by following the time profile of the absorption of e_{aq}^- at 600 nm. The results are given in Figure 1, where the apparent second-order rate constant k_c is plotted as a function of the SDS concentration. The values of k_c are obtained by dividing the measured pseudo-first-order rate constant k_{obsd} (corrected for the background reaction rate of the electron) by the added metal ion concentration.⁹

Since the electron reacts at a slower rate with micelle bound ions^{4,8} than it does with free ions in the bulk solution, k_{obsd} can actually be divided into two terms

$$k_c[A^{n+}]_{tot} = k_{obsd} = k_F[A^{n+}]_F + k_B[A^{n+}]_B \quad (3)$$

(2) (a) K. Kalyanasundaram, F. Grieser, and J. K. Thomas, *Chem. Phys. Lett.*, **51**, 501 (1977); (1977); (b) R. Humphry-Baker, Y. Moroi, and M. Grätzel, *ibid.* **58**, 207 (1978).

(3) V. C. Reinsborough and B. H. Robinson, *J. Chem. Soc., Faraday Trans. 1*, **11**, 2395 (1979).

(4) A. Henglein and Th. Proske, *Ber. Bunsenges. Phys. Chem.*, **82**, 471 (1978).

(5) G. Beck, J. Kiwi, D. Lindenau, and W. Schnabel, *Eur. Polym. J.*, **10**, 1069 (1974).

(6) J. Richards, G. West, and J. K. Thomas, *J. Phys. Chem.*, **74**, 4137 (1970).

(7) M. Grätzel, A. Henglein, and E. Janata, *Ber. Bunsenges. Phys. Chem.*, **79**, 475 (1973).

(8) M. Grätzel and J. K. Thomas, *J. Phys. Chem.*, **78**, 2248 (1974).

(9) Metal ion concentrations other than those shown in the caption of Figure 1 were also used at different SDS concentrations. These results gave, within experimental error, the same values of k_c . This is important because it shows that there are no anomalous effects due to multiply occupied micelles.

Table I. Rate Constants for the Quenching of Excited Pyrene by the Metal Ions Tl^+ and Ag^+ in Water and SDS Solutions

[SDS]/M	$10^{-9}k^a/M^{-1} s^{-1}$	
	Ag^+	Tl^+
0	6.5 ± 0.4	5.0 ± 0.3
0.02	22 ± 3	20 ± 1
0.05	15 ± 3	15 ± 4
0.1	8.6 ± 0.2	9.2 ± 0.7
0.2	6.0 ± 0.2	7.0 ± 0.3

^a Average of three or more concentrations of metal ions in the range 0.2–2 mM.

where the subscripts tot, F, and B refer to the total, free, and bound metal ions,¹⁰ respectively. This equation readily shows that the larger the fraction of micelle bound ions, the smaller k_{obsd} will be and consequently k_c . On the basis of eq 3, the results seen in Figure 1 can be explained.

Consider the data for Tl^+ and Ag^+ . The decrease in k_c with an increase in the SDS concentration is greater than what could be contributed to an ionic strength effect. The change therefore reflects an increase in the fraction of bound ions as the micelle concentration is increased.

The relative small variation in k_c over the surfactant range studied, in comparison to those of the Eu^{3+} and Cu^{2+} systems, indicates that the singly charged ions are not as strongly bound. This conclusion is also consistent with the fluorescence quenching results using these ions, as will be seen in the following section.

For the Eu^{3+} system, the initial decrease in k_c observed at 0.01 M SDS is a factor of almost 80 lower than that in bulk water. This large change indicates that essentially all the Eu^{3+} ions are bound to the SDS micelles. The gradual increase in k_c at higher SDS concentrations is an effect caused by the increase in the ionic strength of the solution. The latter factor reduces the extent of the repulsion potential surrounding the negative micelle which makes it possible for e_{aq}^- to approach the micelle surface to a greater extent and consequently react with adsorbed metal ions. The same effect can be seen when an inert electrolyte is added to the micelle solution.⁸ With a sample of 0.02 M SDS/0.15 M NaCl and 1 mM Eu^{3+} the reaction rate constant was $6.3 \times 10^9 M^{-1} s^{-1}$.

In the case of the Cu^{2+} /SDS system the initial decrease in k_c at low SDS concentrations shows that at about 0.02 M SDS is required to bind all the Cu^{2+} ions. This value is in agreement with what has been measured for other divalent ions with the use of completely different techniques.^{11,12} The increase in k_c at SDS concentrations greater than 0.02 M can be explained in the same way as has been discussed above for Eu^{3+} .

Collectively the data are consistent with a trend one would expect on purely electrostatic considerations. Exact values of the distribution constants cannot, however, be obtained because k_B , $[A^{n+}]_F$, and $[A^{n+}]_B$ are not known with any certainty. Rough estimates that were made give K values of $\sim 10^3 M^{-1}$ for Ag^+ and Tl^+ , $(6-9) \times 10^4 M^{-1}$ for Cu^{2+} ,¹³ and $>10^5 M^{-1}$ for Eu^{3+} .

(II) Quenching of Pyrene Fluorescence by Single Valent Metal Ions in Micellar Solution. The quenching of the pyrene fluorescence by the metal ions Ag^+ and Tl^+ was pseudo-first-order in the surfactant range studied, 0.02–0.2 M SDS. Table I lists

the apparent second-order rate constants obtained at different SDS concentrations.

Before discussing the implications of these observations it is instructive to consider the solubilized pyrene. The results from a recent study,¹⁴ on the solubilization of arenes in micellar solutions, suggest that pyrene is solubilized at or close to the surface of SDS micelles. This means that excited pyrene will be quenched by metal ions adsorbed in the micelle Stern layer. There is no need to invoke¹⁵ the highly improbable "water channels" leading to the micelle core to explain how the excited pyrene and quencher interact. Quenching interactions may also be enhanced because of the dynamic nature of the micelle monomer units. Rapid protrusions¹⁶ of the monomers from the micelle may expose a surface-orientated pyrene to metal ions present in the diffuse counterion region around the micelle surface.

Another aspect of the solubilized pyrene is that the average residence time in SDS micelles is about 0.25 ms,¹⁴ considerably longer than the lifetime of the excited state, 360 ns. Therefore, the events monitored by the fluorescence from excited pyrene all occur with pyrene molecules that have not left the micelles in which they were initially excited.

The observed pseudo-first-order quenching of excited pyrene by Tl^+ and Ag^+ in the micellar solution implies that the metal ions exchange with the intermicellar phase at a rate faster than or comparable with that of the intramicellar quenching rate. Such a case has been treated by Infelta et al.¹⁷ and Infelta¹⁸ for conditions similar to the present situations. Equation 4 describes the

$$I_t = I_0 \exp \left[- \left(k_f + \frac{k_q k^+ [A^{n+}]_{tot}}{(k^- + k_q)(1 + K[M])} \right) t - \frac{K k_q^2 [A^{n+}]_{tot} \{1 - \exp[-(k^- + k_q)t]\}}{(k^- + k_q)^2 (1 + K[M])} \right] \quad (4)$$

time dependence of the fluorescence when the quencher exchanges between micelles and the intermicellar phase, where I_t and I_0 are the fluorescence intensities at time t and $t = 0$, respectively, k_q is the intramicellar quenching rate constant (s^{-1}), and k_f is the reciprocal of the inherent fluorescence lifetime of the micelle-solubilized probe. The other symbols are as defined before.

Under conditions where pseudo-first-order quenching is observed and the rate is linearly dependent on the concentration of the added metal ion, the above equation reduces to eq 5

$$I_t \approx I_0 \exp \left[- \frac{(k_f + k_q k^+ [A^{n+}]_{tot}) t}{(k^- + k_q)(1 + K[M])} \right] \quad (5)$$

or to the logarithmic form of eq 6

$$\ln \left(\frac{I_t}{I_0} \right) \approx - \left(k_f + \frac{k^+ [A^{n+}]_{tot}}{\beta(1 + K[M])} \right) t \quad (6)$$

where

$$\beta = (k^- + k_q)/k_q \quad (7)$$

On the basis of these equations, the second-order constants in Table I can be equated with the second term in brackets in eq 6, i.e.

$$k = k^+/\beta(1 + K[M]) \quad (8)$$

This is particularly useful because a plot of $1/k$ vs. $[M]$ gives an intercept β/k^+ and slope β/k^- and therefore K can be calculated.

(10) Bound ions can be defined here as those that reside in a region between the micelle surface and a distance x away from the charged interface. The point x is where the repulsive potential energy between the micelle and the electron is equal to kT (≈ 25 mV at room temperature). For SDS micelles at low ionic strength x is about 25–30 Å from the micelle surface (see ref 8). The distance from the center of the micelle core to the point x is referred to as the Onsager distance (l).

(11) (a) A. Hasegawa, Y. Michihara, and M. Miura, *Bull. Chem. Soc. Jpn.*, **43**, 3116 (1970); (b) J. Oakes, *J. Chem. Soc., Faraday Trans. 2*, **69**, 1321 (1973).

(12) J. Holzwarth, W. Knoche, and B. H. Robinson, *Ber. Bunsenges. Phys. Chem.*, **82**, 1001 (1978).

(13) This value is somewhat higher than $1400 M^{-1}$ given in ref 8. It should be noted that work in ref 8 was made at 0.1 M SDS, where, as seen from the present work, all Cu^{2+} are bound. Thus the assumptions made in calculating K were not valid.

(14) M. Almgren, F. Grieser, and J. K. Thomas, *J. Am. Chem. Soc.*, **101**, 279 (1979).

(15) M. A. J. Rodgers and M. F. da Silva e Wheeler, *Chem. Phys. Lett.*, **53**, 165 (1978).

(16) G. E. A. Aniansson, *J. Phys. Chem.*, **82**, 2805 (1978).

(17) P. P. Infelta, M. Grätzel, and J. K. Thomas, *J. Phys. Chem.*, **78**, 190 (1974).

(18) P. P. Infelta, *Chem. Phys. Lett.*, **61**, 88 (1979).

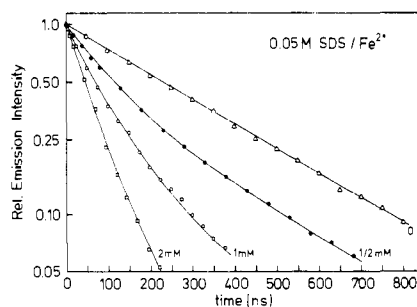


Figure 2. Semilog plots of the fluorescence quenching of excited pyrene as a function of $[\text{Fe}^{2+}]$. The solutions were at a pH of 3.1 (see Experimental Section in text). Time zero is taken at the end of the laser pulse. This applies to the other figures as well.

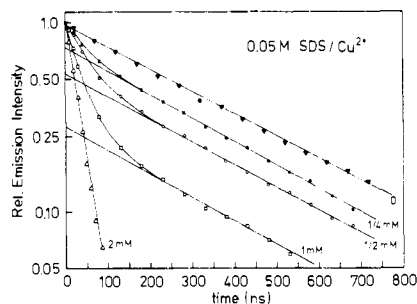


Figure 3. Semilog plots of the fluorescence quenching of excited pyrene in 0.05 M SDS, as a function of $[\text{Cu}^{2+}]$.

The data in Table I were treated in this way, and K values of 1.3×10^3 and $1.1 \times 10^3 \text{ M}^{-1}$ were calculated (15% error limits) for Ag^+ and Tl^+ , respectively. If it is assumed that k^+ is a diffusion-controlled rate constant, the parameters k^- and k_q can also be calculated. The diffusion constant^{4,19} taking into account the electrostatic attraction between the micelle and the metal ion can be expressed by the Debye-Smoluchowski equation (9), where

$$k^+ = \frac{4\pi RDN}{1000} \left[\frac{-l}{R} / \left\{ \exp\left(\frac{-l}{R}\right) - 1 \right\} \right] \quad (9)$$

R and D are sums of the radii and diffusion coefficients, respectively, for the ion plus micelle and N is Avogadro's constant. For Ag^+ and SDS micelles with $R = 20 \text{ \AA}$, $l = 40 \text{ \AA}$,¹⁰ and $D \simeq D(\text{Ag}^+) = 1.7 \times 10^{-5} \text{ cm}^2/\text{s}$,²⁰ one obtains $k^+ = 5.9 \times 10^{10} \text{ M}^{-1} \text{ s}^{-1}$. With this value one calculates $k^- = 4.5 \times 10^7 \text{ s}^{-1}$, $\beta = 2.1$, and hence $k_q = 4.1 \times 10^7 \text{ s}^{-1}$. The values for Tl^+ are, within experimental error, the same.

Although k^+ could not be independently determined, there is other information which suggests that the calculated value is a reasonable number. The value of the intercept β/k^+ multiplied by k^+ must give a value of β greater than one (see eq 7). From the experimental values of the intercept this implies that k^+ is greater than $2.9 \times 10^{10} \text{ M}^{-1} \text{ s}^{-1}$. Also, the kinetic conditions that would give pseudo-first-order quenching behavior require that k^- be at least comparable to k_q , and therefore β approaches 2 and k^+ , the values used in the above calculations.

(III) Quenching of Pyrene Fluorescence by Multivalent Metal Ions in Micellar Solution. The divalent metal ions Fe^{2+} , Mn^{2+} , Ni^{2+} , and Cu^{2+} all showed quenching of the pyrene fluorescence in micellar solution; however, the kinetics was no longer first order and varied with both the micelle concentration and the metal ion.

The intensity-time profiles of the quenching curves that were obtained with the ions Mn^{2+} and Fe^{2+} were about the same. Figure 2 shows the time dependence of the pyrene fluorescence as a function of $[\text{Fe}^{2+}]$. The nonlinear semilog plots indicate that Fe^{2+} ions are bound to the micelles to a stronger extent than either

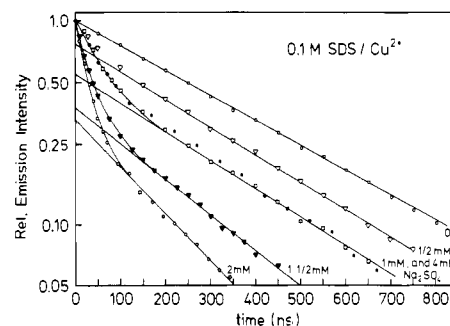


Figure 4. Semilog plots of the fluorescence quenching of excited pyrene in 0.1 M SDS, as a function of $[\text{Cu}^{2+}]$. The solid circular points are for a 1 mM Cu^{2+} SDS sample to which 4 mM Na_2SO_4 had been added.

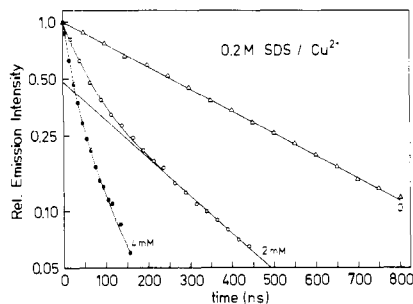


Figure 5. Semilog plots of the fluorescence quenching of excited pyrene in 0.2 M SDS, as a function of $[\text{Cu}^{2+}]$.

Ag^+ or Tl^+ but exchange from micelle to micelle still occurs in a time range comparable with the lifetime of the probe. How this exchange occurs, whether by the equilibrium sequence i-ii or by reaction 2, is not clear from these data. The question can be better answered from the results of the Cu^{2+} quenching curves.

For the Cu^{2+} /SDS system a considerable change in the time profile of the fluorescence quenching curves was observed as a function of both the SDS and Cu^{2+} concentration. These data are presented in Figures 3-5. The semilog plots show a distinct two part kinetic form at low SDS concentrations and eventually change into the nonexponential decays, shown for the Fe^{2+} /SDS system, at 0.2 M SDS.

For strongly bound ions which are distributed among the micelles according to Poisson statistics, the kinetics form of the fluorescence decay can be described by eq 10^{15,16,21} or by the logarithmic form (11) where $\bar{n} = [\text{A}^{n+}]_{\text{tot}}/[\text{M}]$, $[\text{M}] = ([\text{surfactant}] - \text{cmc})/\bar{N}$, and \bar{N} is the aggregation number.

$$I_t = I_0 \exp[\bar{n}(e^{-k_q t} - 1) - k_f t] \quad (10)$$

$$\ln \left(\frac{I_t}{I_0} \right) = \bar{n} (e^{-k_q t} - 1) - k_f t \quad (11)$$

Equation 1 predicts a two-component decay of the fluorescence signal: a fast decay at short times corresponding to micelles occupied by a probe and quencher(s), and a slow component equal to k_f at longer times due to micelles with a probe only. This agrees with the curves observed at $[\text{Cu}^{2+}] \leq 1 \text{ mM}$ in Figures 3 and 4.

The change in the slope of the slower component in Figures 4 and 5 at $[\text{Cu}^{2+}] > 1 \text{ mM}$ is not accounted for by eq 11. Nor can the change be explained by effects caused by a small change in the ionic strength of the solution. The addition of 4 mM Na_2SO_4 to 1 mM Cu^{2+} /0.1 M SDS gave the same curve as that observed for 1 mM Cu^{2+} /0.1 M SDS (see Figure 4). Furthermore, all the Cu^{2+} ions are bound at the SDS concentrations at which the effects are observed. Considering all these points, a reasonable explanation of the results could be described in terms of bound metal ion exchange through micelle-micelle collisions (reaction 2). Further evidence to support this suggestion was found in some related experiments and calculations.

(19) A. J. Frank, M. Grätzel, A. Henglein, and E. Janata, *Ber. Bunsenges. Phys. Chem.*, **80**, 547 (1976).

(20) Landolt and Börnstein, "Transport Phenomena I", 6th ed., Part 5, Springer-Verlag, 1969, pp 631-633.

(21) S. S. Atik and L. A. Singer, *Chem. Phys. Lett.*, **59**, 519 (1978).

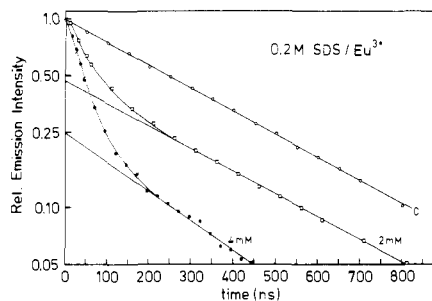


Figure 6. Semilog plots of the fluorescence quenching of excited pyrene in 0.2 M SDS, as a function of $[Eu^{3+}]$.

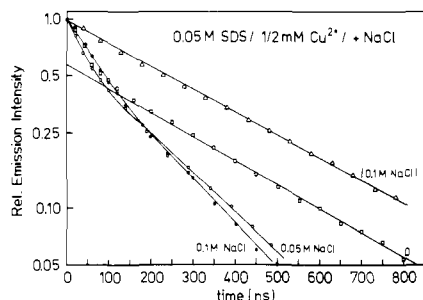


Figure 7. Semi-log plots of the fluorescence quenching of excited pyrene in 0.05 M SDS with 1–2 mM Cu^{2+} in the presence and absence of NaCl. The inherent fluorescence decay of excited pyrene in the presence of 0.1 M NaCl is also shown.

It would be expected that the "tighter" the binding of the adsorbed ion, the less probable would be the exchange by micelle-micelle collisions. This was tested by using the trivalent ion Eu^{3+} . Throughout the surfactant range 0.05–0.2 M SDS, with $[Eu^{3+}]$ the same as for the Cu^{2+} /SDS system, the slow portion of the decay stayed essentially constant and equal to k_f . Figure 6 shows the quenching curves at 0.2 M SDS which should be compared with those of Figure 5.

It may also be argued that the closer the surfaces of two micelles can approach each other during the collision–repulsion process, the greater would be the metal ion exchange rate. This is because the distribution of bound ions is weighted toward the higher potential at the micelle surface and, therefore, there is a greater probability of having a metal ion transfer during the "closer" collision.

A way of attaining a closer approach of the micelle surfaces in a collision is to reduce their surface potential. This can be done by adding an inert salt.²²

Figure 7 shows the effect of adding NaCl on the fluorescence decay curves in the Cu^{2+} /SDS system. As can be seen, in the presence of salt there is a considerable enhancement of the decay rate of the slower component, a trend which follows the predicted behavior discussed above.

These results, however, should also be considered in another light. An ESR study^{11a} on Mn^{2+} binding to SDS micelles indicated that the strength of the Mn^{2+} binding decreased with addition of either $NaNO_3$ or KNO_3 to the micellar solution. It is possible that this decrease in binding is due to two factors. One is that as the potential of the surface decreases, the attraction for the counterion lessens as suggested by the normal Boltzmann equation. The other possibility is that there is a specific exchange of the bound metal ion with the added cation. Such a process was suggested from the results of a study²³ on Tb^{3+} binding to SDS micelles. The important point is that a decrease in the binding means that the equilibrium of the bound ions will be shifted away from the micelle surface and the amount of "free" Mn^{2+} would increase.

In view of this information the results of the fluorescence quenching experiments in the presence of salt do not lead to an

Table II. Calculated Values of the Micelle–Micelle Collisional Ion Exchange Constant k_e in Cu^{2+} /SDS Systems

soln ^a	10^{-6} slope ^b / s^{-1}	$10^{-9} k_e /$ $M^{-1} s^{-1}$
1.5 mM Cu^{2+} /0.1 M SDS	3.3	2.8
2 mM Cu^{2+} /0.1 M SDS	4.9	3.3
2 mM Cu^{2+} /0.2 M SDS	4.1	4.0

^a See ref 26. ^b Corrected for k_f ($2.8 \times 10^6 s^{-1}$).

unequivocal interpretation. If the added salt does cause a significant change in the distribution of Cu^{2+} bound to the micelle, an enhancement of the decay rate of the slower component in the fluorescence curves would be expected. Since we do not have any information on the extent of these salt affects, some caution should, therefore, be taken in interpreting the results of Figure 7.

Support for the collisional ion-exchange process is also found from a quantitative analysis of the data of the Cu^{2+} /SDS system.

The equation describing the fluorescence quenching by metal ions in micellar solution, which includes the collisional exchange process, was published during the course of the present work. Dederen et al.²⁴ extend eq 4 to eq 12,

$$\ln \left(\frac{I_t}{I_0} \right) = -At - B\{1 - \exp[-(k_q + k_e[M] + k^-)t]\} \quad (12)$$

where

$$A = k_f + \frac{k_q(k^+ + k_eK[M])[A^{n+}]_{tot}}{(1 + K[M])(k^- + k_e[M] + k_q)} \quad (13)$$

and

$$B = \frac{(k^+ + k_eK[M])[A^{n+}]_{tot}k_q^2}{(1 + K[M])(k^- + k_e[M])(k^- + k_e[M] + k_q)^2} \quad (14)$$

The slow component of the fluorescence decay in Figures 4 and 5 can be equated with eq 13. For those plots shown where the decay was significantly greater than the inherent fluorescence decay of excited pyrene, the collisional exchange constant k_e was calculated. The results are presented in Table II. In these calculations $k_q = 1.1 \times 10^7 s^{-1}$ (see section V), $K = 6 \times 10^4 M^{-1}$, $k^+ = 2.9 \times 10^{10} M^{-1} s^{-1}$,²⁵ and $k^- = 4.8 \times 10^5 s^{-1}$. The column headed slope lists the measured pseudo-first-order decay constants corrected for the inherent fluorescence lifetime of pyrene (360 ns).

Some indication of the validity of the numbers in Table II can be obtained if we consider the diffusion constant of colliding micelles calculated by using the Smoluchowski equation, $k_D = 4\pi RDN/1000$. The diffusion coefficient for SDS micelles is about $1 \times 10^{-6} cm^2/s$,²⁷ and the radius of the diffuse charge cloud at the point where the repulsion potential is about equal to the thermal energy is 40–45 Å (see ref 10). (Note: this is the sum of the micelle radius (~ 16 Å) plus the diffuse layer thickness, to the point where the micelle potential is ~ 25 mV.) Thus, with $R = 80$ – 90 Å (the sum of the interacting radii) and $D = 2 \times 10^{-6} cm^2/s$ (the sum of the diffusion coefficients of the colliding spheres), $k_D = (1.2$ – $1.4) \times 10^{10} M^{-1} s^{-1}$. This value can be considered an upper limit. As the micelles approach each other and the distance between their centers becomes less than 80–90 Å, there will be a greater overlap of the diffuse charge layers and a concomitant increase in the repulsion between the micelles. Therefore, the collision-exchange constant would be expected to be lower than the theoretical upper limit. The experimentally

(24) J. C. Dederen, M. Van der Anweraer, and F. C. deSchryver, *Chem. Phys. Lett.*, **68**, 451 (1979).

(25) The value of k^+ was calculated by using eq 11 with $R = 20$ Å, $D_{Cu^{2+}} = 0.6 \times 10^{-5} cm^2/s$ (ref 20), and $l = 50$ Å (estimated from the curve in ref 8, making allowance for the fact that Cu^{2+} is bivalent).

(26) The micelle concentrations were calculated by using the equation $[M] = ([surfactant] - cmc)/N$. The value of N was taken as 62 for 0.05 and 0.1 M SDS and as 70 for 0.2 M SDS (M. Almgren, F. Grieser, and J. K. Thomas, *J. Am. Chem. Soc.*, in press).

(27) F. Tokiwa and K. Ohki, *J. Phys. Chem.*, **71**, 1343 (1967).

(22) M. S. Fernandez and P. Fromherz, *J. Phys. Chem.*, **81**, 1755 (1977).

(23) F. Grieser, submitted for publication in *J. Phys. Chem.*

obtained constant which is ~ 4 times lower than the theoretical limit can therefore be considered a reasonable value.

It should be pointed out that the ions that exchange in the collision are predominately the bound ions (see ref 10) which reside in the outer regions of the diffuse layer and not those which are close to the micelle Stern layer.

The exchange constant obtained in the present work can also be compared to that given in a recent study involving the dynamics of Eu^{2+} bound to SDS micelles. Moroi et al.²⁸ considered the movement of Eu^{2+} (formed by an electron-transfer reaction from excited methylphenothiazine to Eu^{3+}) among SDS micelles and gave a detailed analysis of the kinetics involved. The reaction mechanism they described included a collisional exchange step for Eu^{2+} and indicated that their data supported such an assignment, with a rate constant of $2.6 \times 10^9 \text{ M}^{-1} \text{ s}^{-1}$. This value is quite consistent with our Cu^{2+} /SDS calculations given in Table II.

Collectively, the above information shows that the interpretation of the fluorescence quenching curves in the presence of Cu^{2+} , and possibly for the other bivalent metal ions,²⁹ in terms of a collisional ion-exchange process is a plausible explanation.

One final remark we wish to make on the calculated k_e values is in relation to the work of Dederen et al. These workers also calculated an exchange constant for Cu^{2+} , on the basis of computer fitting analyses of fluorescence quenching curves from 1-methylpyrene in SDS/ Cu^{2+} solutions. The value they quoted was $6 \times 10^8 \text{ M}^{-1} \text{ s}^{-1}$, which is significantly lower than the values given in Table II. The main reason for the discrepancy appears to lie with the values of k^+ and K used. In the work of Dederen et al. these two constants were treated as changeable parameters and adjusted to give the best fit to the experimental results. The values that gave an acceptable fit were quoted as $k^+ = 1.2 \times 10^9 \text{ M}^{-1} \text{ s}^{-1}$ and $K = 10^4 \text{ M}^{-1}$.

It is most unlikely that k^+ could be as low as this value. Although we are not aware of a direct measurement of k^+ for a metal ion, there are measurements of this parameter for the neutral molecules CH_2I_2 ¹⁷ ($k^+ = 2.5 \times 10^{10} \text{ M}^{-1} \text{ s}^{-1}$) and 1-bromonaphthalene¹⁴ ($k^+ = 7 \times 10^9 \text{ M}^{-1} \text{ s}^{-1}$) entering SDS micelles. Further justification in using k^+ as a diffusion-controlled parameter has already been discussed earlier for the Ag^+ and Tl^+ systems.

The value of the equilibrium constant used by Dederen et al. also seems too low. A value of 10^4 M^{-1} would not be compatible with the electron rate data for the Cu^{2+} system given in Figure 1.

On the basis of the above remarks the values given in Table II are probably better estimates of k_e for the Cu^{2+} /SDS system than those given by Dederen et al.; however, since the uncertainty in K remains, they can still be regarded as only approximate.

(IV) **Intramolecular Fluorescence Quenching by Cu^{2+} and Eu^{3+} .** The quenching interaction of two species within a micelle has been recognized for a variety of probes and quenchers.^{17,30-32} The limiting slope, at short times, of the semilog plots of the fluorescence intensity such as in Figures 3 and 4 at Cu^{2+} concentrations less than or equal to 1 mM can be related to the intramolecular quenching constant k_q . This is seen from the reduced form of eq 11, which, when t is small, becomes eq 15.

$$\ln \left(\frac{I_t}{I_0} \right) = -((k_f + \bar{n}k_q)t) \quad (15)$$

(28) Y. Moroi, P. P. Infelta, and M. Grätzel, *J. Am. Chem. Soc.*, **101**, 573 (1979).

(29) For the Ni^{2+} /SDS system, at 0.05 M SDS two-component decays were observed with the slower part becoming fast at higher ion concentrations much like the Cu^{2+} data at 0.1 M SDS. From the data in ref 12, it would be expected that all the Ni^{2+} ions ($\leq 1.5 \text{ mM}$) would be bound at 0.05 M SDS.

(30) S. S. Atik, M. Nam, and L. A. Singer, *Chem. Phys. Lett.*, **67**, 75 (1979).

(31) S. S. Atik and L. A. Singer, *Chem. Phys. Lett.*, **66**, 234 (1979).

(32) G. Rothenberger, P. P. Infelta, and M. Grätzel, *J. Phys. Chem.*, **83**, 1871 (1979).

(33) The micelle concentration for $\text{C}_{12}(\text{EtO})_3\text{S}$ was calculated by using a $\text{cmc} = 1 \times 10^{-4} \text{ M}$ and $N = 60$ (see section V of text).

(34) The value are the average of three determinations in pyrene-saturated water ($\sim 5 \times 10^{-7} \text{ M}$). The lifetime of pyrene in water was 140 ns.

Table III. Rate Constants for the Intramolecular Quenching of Excited Pyrene by Cu^{2+} and Eu^{3+} Ions

soln	Cu^{2+}		Eu^{3+}	
	\bar{n}	$10^{-6}k_q^a / \text{s}^{-1}$	\bar{n}	$10^{-6}k_q^a / \text{s}^{-1}$
0.05 M SDS	0.34, 0.67, 1.34	12 ± 1	0.34, 0.67, 1.34	8.7 ± 0.3
0.1 M SDS	0.32, 0.65	11 ± 1	0.65, 0.97, 1.3	9.3 ± 0.3
0.2 M SDS			0.62, 1.26	8.6 ± 0.3
0.05 M $\text{C}_{12}(\text{EtO})_3\text{S}^{\delta}$	0.6, 0.87, 1.17	8.1 ± 0.2	0.53, 0.77, 0.85	4.3 ± 0.3
water ^c		$(4.8 \pm 0.2) \times 10^9 \text{ M}^{-1} \text{ s}^{-1}$		$(1.3 \pm 0.1) \times 10^9 \text{ M}^{-1} \text{ s}^{-1}$

^a Calculated from eq 15 by using $k_f = 2.8 \times 10^6 \text{ s}^{-1}$. ^b See ref 33. ^c See ref 34.

The intramolecular quenching constants obtained (on the basis of eq 15) for the quenching of pyrene fluorescence by Cu^{2+} and Eu^{3+} ions in SDS and $\text{C}_{12}(\text{EtO})_3\text{S}$ solutions are given in Table III. It can be seen that within experimental error, the k_q values remain constant with both a change in \bar{n} and the SDS micelle concentration, for both metal ions. Indeed this is what one would expect if the interaction was in a fixed, localized volume and was independent of any effects due to multiple occupancy by quencher molecules. When the micelle volume is changed, however, as with the $\text{C}_{12}(\text{EtO})_3\text{S}$ surfactant, a noticeable change in k_q is seen. The change could be due to a shift in the average position of solubilization of the pyrene molecule in the micelle compared to those in SDS micelles. Even if this was not the case and pyrene was still largely at or near the surface, the larger radius of $\text{C}_{12}(\text{EtO})_3\text{S}$ micelles means that the volume of the outer shell has increased, and consequently one would expect a lowering in k_q .

The data in Table III also show that Cu^{2+} is slightly more efficient than Eu^{3+} in quenching excited pyrene in SDS micelles and is better by a factor of almost 2 in $\text{C}_{12}(\text{EtO})_3\text{S}$ micelles. This difference may be partly due to the inherently greater quenching capacity of Cu^{2+} , as is seen in the data obtained for free solution (Table III). This statement would also be consistent with the higher k_e value calculated for Ag^+ . However, it cannot be the only aspect influencing the reaction rate since the relative difference between the rate constants in the micelles is not as great as it is in free solution. As mentioned earlier such factors as steric hindrance by the micelle head groups and orientation limitations in probe-quencher interactions must affect the quenching rates and these factors may be somewhat different for the two ions. The "tightness" of the binding in the Stern layer between Eu^{3+} and Cu^{2+} could also have some influence on the ultimate rates of interaction with the solubilized probe. The extent of these effects and their variation between the two ions cannot be extracted from the present data; only that they exist is noted in the differences in the k_q values.

(V) **The Statistical Distribution of Metal Ions in Micellar Solutions.** All the equations which have been used in evaluating the fluorescence data have been derived by assuming that both the metal ions and pyrene molecules are scattered among the micelles in the form of a Poisson distribution. That the distribution of hydrophobic molecules among micelles follows Poisson statistics has been amply shown.^{14,32} That quasi-bound metal ions also follow such a distribution can be shown from the two-part quenching curves as seen in Figures 2-4.

If probe molecules and metal ions are both distributed among micelles in the form of a Poisson distribution, then the ratio of micelles with both probe and metal ion(s), MPA^{n+} , to those with a probe only, MP, is given by eq 16. This ratio is directly related

$$f = \frac{[\text{MPA}^{n+}]}{[\text{MP}]} = e^{[A^{n+}]_{\text{tot}}/[M] - 1} \quad (16)$$

to the relative proportion of quenched to unquenched probes in systems where the bound ions are quasi-static. These relative

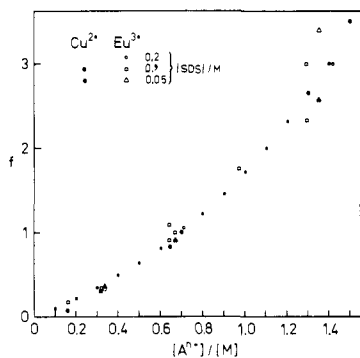


Figure 8. The ratio, f , of the relative proportion of quenched probes to unquenched in metal ion/SDS solutions is plotted, as a function of $[A^{2+}]/[M]$. The points are calculated from eq 16, which assumes that the probes and quasi-static metal ions are both distributed among the micelles following Poisson statistics.

proportions³⁵ can be obtained from the semilog plots as in Figures 3, 4, and 6. By extrapolating the longer lived decay back to zero, we obtained the relative proportion of unquenched probes and consequently the fraction that is quenched. Note, this is only valid for the curves which are minimally affected by the micelle-micelle collisional-exchange process.

In Figure 8, experimental f values have been plotted against $[A^{2+}]_{tot}/[M]$ and compared with those of the expected curve based on 16. As can be seen, the agreement is quite good and gives independent support for the Poisson distribution for metal ions

(35) Time zero for the emission quenching plots is taken at the end of the laser pulse. This introduces some error into the calculation of the relative proportions because quenching of the fluorescence signal occurs during the finite (~ 25 ns at 10% of pulse height) duration of the pulse. However, this is relatively small in the range of $[A^{2+}]/[M]$ ratios studied.

bound to micelles in a quasi-static state.

This could be shown equally well from eq 17, the reduced form of eq 11, which has a linear approximation at large values of t . Extrapolation of the slower linear component such as in Figure 3 gives at $t = 0$ an intercept equal to $-\bar{n}$.

$$\ln \left(\frac{I_t}{I_0} \right) = -(\bar{n} + k_f t) \quad (17)$$

By applying these last two equations to calculate the aggregation number of $C_{12}(EtO)_3S$ micelles, we obtained a value of 56 ± 5 . This value compares favorably with that of 61 ± 2 obtained by the Turro and Yekta method.³⁶

Summary and Conclusions

The fluorescence quenching data clearly shows that the more highly charged the metal ion the greater is its tendency to bind to the micelle surface, as one would expect on purely electrostatic considerations. This conclusion is also supported by the data obtained from the reaction rates of the hydrated electron in metal ion/SDS solutions. The strength of metal ion binding to SDS micelles, suggested by the pyrene fluorescence quenching results, follows the order $Eu^{3+} > Cu^{2+} > Ni^{2+} > Mn^{2+}, Fe^{2+} > Tl^+, Ag^+$.

Evidence for the migration of bound metal ions through micelle-micelle collisions has also been found from the characteristics of the fluorescence quenching curves. It is found to be relatively fast at high micelle concentrations. Thus it is a process that should not be neglected when metal ion reactions in micellar systems are interpreted, particularly over an expanded micelle concentration range.

Experimental support that the distribution of strongly bound metal ions (i.e., bound during the lifetime of the excited pyrene) follows Poisson statistics has also been found.

(36) N. J. Turro and A. Yekta, *J. Am. Chem. Soc.*, **100**, 5951 (1978).

Determination of Rate Constants for Photosolvation Reactions: Solvent Dependence of Chloride Substitution Rates for Excited States of *cis*-Dichlorobis(2,2'-bipyridine)iridium(III)

B. Divisia,¹ P. C. Ford,* and R. J. Watts*

Contribution from the Department of Chemistry, University of California, Santa Barbara, California 93106. Received April 30, 1980

Abstract: Emission quantum yields, lifetimes, and spectra as well as photosolvation yields have been determined for *cis*-dichlorobis(2,2'-bipyridine)iridium(III), $IrCl_2(bpy)_2^+$, and its deuterated analogue $IrCl_2(bpy-d_8)_2^+$ in water, methanol, dimethylformamide, and acetonitrile. Both charge-transfer and ligand-field excited states contribute to the decay properties in fluid solutions. Rates of photosolvation are strongly solvent dependent, consistent with a dissociative or dissociative interchange mechanism. Rates of radiationless decay are also strongly solvent dependent as are the intensity distributions in the emission spectra. Upward movement of the charge-transfer state in water solutions accounts for the large contribution of the ligand-field emission in this solvent relative to nonaqueous media.

I. Introduction

The rate constants and mechanistic details of a vast number of thermal ligand substitution processes in transition-metal complexes have been studied and established with some certainty.²

(1) On leave from the Laboratoire DRF/EDA, Center d'Études Nucléaires de Grenoble, 85 × 38041 Grenoble Cedex, France.

(2) (a) Wilkins, R. G. "The Study of Kinetics and Mechanism of Reactions of Transition Metal Complexes"; Allyn and Bacon: Boston, Mass., 1974; Chapter 4. (b) Basolo, F.; Pearson, R. G. "Mechanisms of Inorganic Reactions", 2nd ed.; Wiley: New York, 1967; Chapters 3 and 5.

While it is clear that the ligand-field excited states of low-spin d^6 complexes are far more labile toward ligand substitution than are the ground states,³ interpretation of this enhanced lability has been hampered by a dearth of quantitative kinetic data, stemming from inherent difficulties in the measurement of excited-state lifetimes under conditions relevant to the photochemistry. Several notable exceptions include determinations of rate constants for

(3) Balzani, V.; Carassiti, V. "Photochemistry of Coordination Compounds"; Academic Press: London, 1970.